Seventh International Conference on Control, Automation, Robotics And Vision (ICARCV'02), Dec 2002, Singapore

Quantifying Skull Shape

JAMES DEVENISH[1], ROBERT LINGGARD[2], KASIA MICHALAK[2], KRIS PARKER[2], IRINA EMELYANOVA[2], LESLEY CALA[1] YIANNI ATTIKIOUZEL[2], NEIL HICKS[3], PETER ROBBINS[4], FRANK MASTAGLIA[5]

devenish@arcme.com, bobling@arcme.com, lesacala@iinet.net.au

[1]Australian Research Centre for Medical Engineering (ARCME), The University of Western Australia, 35 Stirling Hwy, Crawley, WA 6009 Australia
[2]ARCME, Murdoch University, South Street, Murdoch, WA 6150 Australia
[3]Sir Charles Gairdner Hospital, Verdun St, Nedlands, WA 6009 Australia
[4]The West Australian Centre for Pathology and Medical Research (PathCentre), Hospital Ave, Nedlands, WA 6009 Australia
[5]Centre for Neuromuscular and Neurological Disorders, The University of Western Australia

Abstract: This paper describes a technique for automatically quantifying the shape of the skull cavity seen on an axial slice in a CT brain scan. The development of this algorithm derives from the need to normalise CT scan data according to skull size and shape for the purpose of comparing new patient data with that from past cases. This algorithm uses image processing techniques to find the inner edge of the bones of the skull on an axial slice, so that its shape can be represented by a radius function. A simple measure of shape asymmetry is defined. It is also shown that this shape can be quantified more precisely by harmonic analysis using the Fourier Transform of the radius function. This paper describes the design of the algorithm and its performance on axial slices taken from a database of CT brain scans from 528 patients.

Key Words: human brain shape, CT head scanner, skull measurement, normalisation, shape analysis, Fourier series, morphometry, grey level imaging (GLI).

1 Introduction

The main motivation for this research work comes from a wish to provide a diagnostic aid to radiologists interpreting CT brain scans. It is desirable that the CT data from a new patient be comparable with that from past cases in order to take advantage of previously successful diagnoses. Normalisation may enable automated pattern recognition as well as increased objectivity of analysis [1].

This paper deals with the problem of quantifying the shape of the skull cavity and defines some measures of shape asymmetry. The basis of our algorithm is the successful extraction of an outline from axial CT scans. The normalisation of shape is particularly difficult since it is not a one-dimensional parameter and varies from case to case. This paper demonstrates how shape can be approximated using Fourier series.

We developed unsupervised analysis software (in the Java language) and used it to process 528 cases.

2 Axial Scan Images

In a previous paper, we described a method of measuring brain height automatically [2]. The measurement of brain height allows us to find the anatomical level of each axial slice in an image stack.

Data sets for this study were obtained from pre-existing studies at Sir Charles Gairdner Hospital, under Human Research Ethics Committee trial number 2000-136 issued to Adjunct Professor Lesley Cala (L.C.). All scans were made on living patients with or without focal abnormalities. Images were obtained as transverse (axial) slices with varying thickness of 3–6 mm with 512×512 pixel sets. We only used images without contrast media. Additionally, each axial series was accompanied by a lateral scout (view showing skull from the side) for localisation of the slices.

In order to standardise the position at which we will measure skull shape, we have chosen to use an anatomical level 37% of the distance along a line drawn perpendicular to the orbitomeatal line (outer corner of the eye to the ear hole) and terminating at the inner table of the skull vault. This is the position of the connection between the thalamus on each side and 'bi-parietal diameter,' where the width of the skull is usually measured. A typical axial image at this level is shown in Figure 1.

3 Detecting the Inner Cavity Shape

The shape that we sought to quantify was delimited by the inner bone contour of the skull. Since the brain occupies most of the cranial volume, we used the bone contour as a proxy for transverse cross-sections of the brain. Differentiation of bone from brain tissue was accomplished by a threshold at 200 Hounsfield units. Bone appears white in Figure 2 and so does some additional physiological cal-

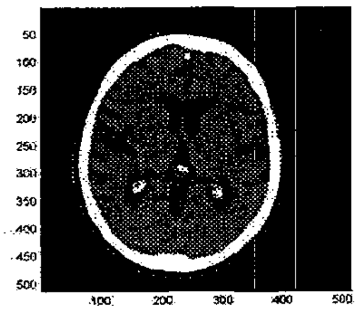

Figure 1: *Axial Scan* A typical 512 × 512 pixel axial CT brain scan at the level of the bi-parietal diameter, showing brain tissue surrounded by bone.

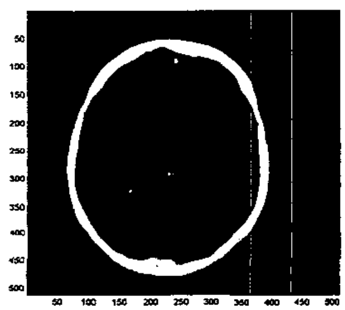

Figure 2: The CT brain scan of Figure 1, posterised with a threshold at 200 H, clearly demarcates the skull from the surrounding tissue. The threshold also picks up some calcification within the brain.

cification within the brain.

The inner edge of the skull can be sampled by an edge following algorithm. The result of this is the simply-connected closed contour (outline) shown in Figure 3. This set of samples—the shape we measured and quantified—will be referred to as a shape boundary.

3.1 Finding the Axis of Least Asymmetry

In order to make direct comparisons between different shape boundaries, it is necessary to have all shape boundaries aligned in a standard way. The standard orientation that has been chosen is with the axis of longitudinal symmetry vertically "upright" in a rectangular image frame. This axis of symmetry notionally bisects the brain. Some difficulty lies in the fact that the shape boundary is never perfectly symmetrical in reflection or rotation. A compromise is to determine the axis of least asymmetry. This is found by calculating a measure of asymmetry for several axes and choosing the axis with least asymmetry. In a companion paper (Michalak, in these proceedings) we describe in detail how this operation is performed. After adjustment, the shape boundary appears like Figure 4.

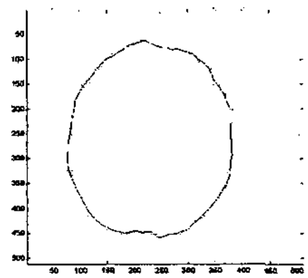

Figure 3: The shape boundary from Figure 2, unadjusted.

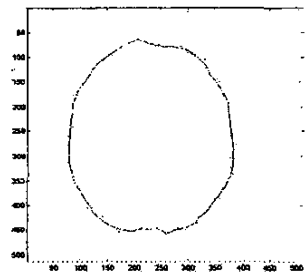

Figure 4: *Straightened Shape Boundary* The shape boundary from Figure 2, rotated 3.7° about its centroid so that the axis of least asymmetry is vertical.

4 Sampling Shape Boundaries

In quantifying brain shape, we investigated Fourier descriptors to find non-localised qualities of inner cavity shape. (Large local features were only expected to arise from bone abnormalities or the location of the inter-hemispheric fissure and were not of interest in describing general 'cavity shape'.) Radial point-coordinate samples were preferred because of their directness and obvious ties with Fourier series analysis. Advantages of Fourier analysis include the small number of descriptors and the separability of translation, dilation, and rotation. Fourier series can also offer robustness in the presence of noise [3].

As in Anstey (1973) [4], we choose the centroid as the origin for polar coordinates. It was found, by manual examination, that 1024 equally-spaced radial samples were sufficiently accurate to describe the inner bone edge at the bi-parietal diameter. Equal angular spacing over 2π (periodic) radians greatly eases Fourier analysis [5]. It was also necessary to find some fiducial points at which sampling is aligned (this prevents the appearance of phase dependencies in subsequent analysis). The frontal intersection of the axis of least asymmetry was used (see Figure 5).

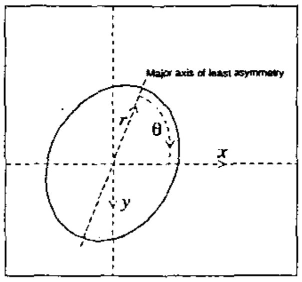

Figure 5: *Normal Coordinate System* For an arbitrary image (solid lines), a normal coordinate system is found. The centroid of the bounded shape is used as the origin and Cartesian or polar coordinates are measured to be increasing in the directions shown by arrows. The angular origin is the axis of least asymmetry.

5 Measuring Asymmetry

If the shape boundary were perfectly symmetrical, then its radius function would be the same if it were reversed—that is, if the shape boundary were flipped about its axis of symmetry. A simple measure of asymmetry is, therefore, the sum of squared differences between the radius function and its reflection. However, such a measure would depend on the overall size of the skull. To obtain a normalised value of asymmetry, the sum of squares is divided by the square of the average radius. For set of radial samples $R = \{r_1, \ldots, r_{1024}\}$, the asymmetry is measured as:

$$\frac{\sum_{n=1}^{1024}\left(r_n - r_{1025-n}\right)^2}{\left(\frac{1}{1024}\sum_{n=1}^{1024} r_n\right)^2}$$

We call this the degree of asymmetry of a shape boundary. The shape boundary in Figure 4 has a degree of asymmetry of 0.3288. This degree of asymmetry will later be used for shape classification.

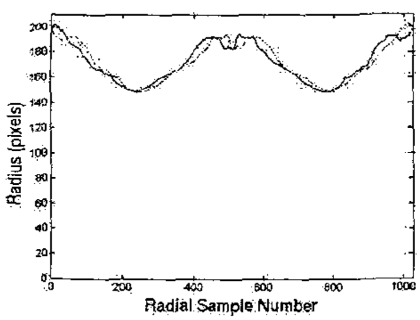

Figure 6: *1024-sample Radius Function* The radius function of the shape boundary shown in Figure 4. Its reflection is overlaid on the plot.

6 Quantifying Shape

The radius function of a shape boundary that is aligned along its axis of symmetry can be used to compare and quantify the actual shape. If the shape were a perfect circle, the radius function would have a constant value, equal to the radius of the circle. If the shape were perfectly symmetrical, then the radius function would be an even function, and its Fourier transform would contain only cosine components. A shape that is asymmetrical will have a Fourier transform with both sine and cosine components, and this is the general case. By taking the Fourier transform of the radius function, we can derive a description of its shape using harmonic coefficients.

Figure 7 shows the sine and cosine transform coefficients of the radius function shown in Figure 6, for up to 50 harmonics.

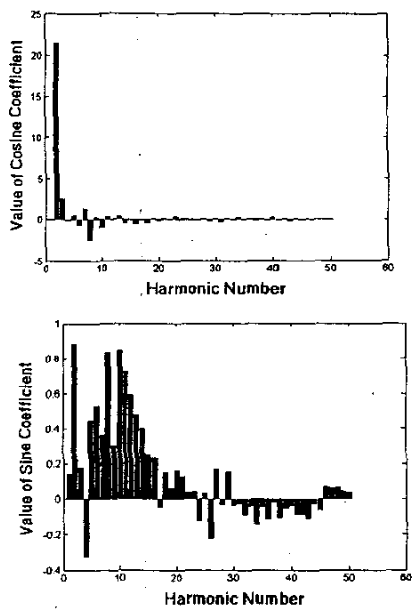

Figure 7: *Harmonic Content of Normalised Shape Boundary* The spectrum of the normalised shape from Figure 4, up to 50 coefficients.

The harmonic series of sine and cosine components extends from zero (a basic circle) up to harmonic number 512. This full series is an equivalent representation of the radius function, since each may be derived from the other. However, if the harmonic series is truncated at a low harmonic number, then we have an approximate representation of the shape boundary. For example, with no harmonics, the approximate shape is a circle.

By taking the sum of squared differences between the actual and approximated radius function, we can estimate a percentage error. This is shown in Figure 8 for up to 50 harmonics (both sine and cosine). The results illustrate that gross shape is fairly well represented with ten harmonics (five sine and five cosine). It has previously been noted that 21 coefficients can be sufficient for some biological characterisation and that spectral power drops rapidly after seven coefficients [6]. It has also been shown that a small number of coefficients can be adequate for image matching purposes [5]. Figure 7 supports these notions for typical brain shape.

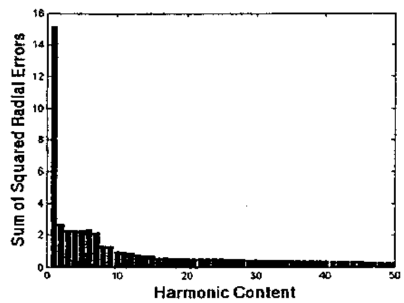

Figure 8: Sum of squared differences between the actual and modelled radius function, for up to 50 harmonics.

If we use only cosine harmonics, then the approximation has perfect bilateral symmetry. The high-frequency harmonics contribute the 'roughness' of the shape boundary while most of the overall shape is described by low-frequency harmonics. Figure 9 demonstrates the contributions of sine and cosine harmonics.

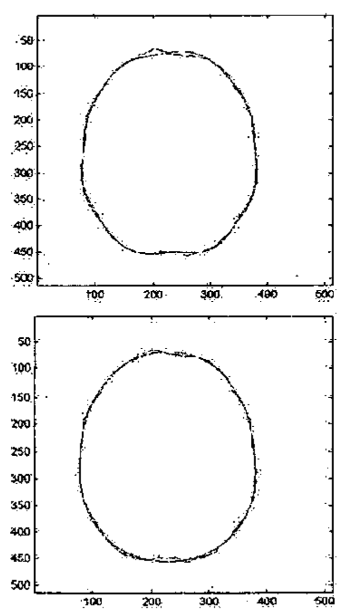

Figure 9: *Low-frequency Harmonic Reconstruction* This shows the accuracy of three sine and three cosine harmonics (first image) and of three cosine components only (following image).

6.1 Curvature Landmarks

Our Fourier analysis provides a superposition of pure cosine waves that describe shape boundaries. The use of low-frequency harmonics results in a 'smooth' shape boundary and provides robustness in the presence of noise. Therefore, it is simple to find local maxima and minima (extrema) of curvature. It is typical that a brain shape boundary will contain several curvature extrema and that these mathematical quantities will correspond to areas such as the frontal poles, occipital poles, and the lateral edges of the brain. It is possible to quantitatively measure the position and magnitude of the curvature extrema for classification purposes.

6.2 Problem Scenarios

The interpretation of this shape analysis is only well defined for the bulk of nil focal cases (as diagnosed by L.C.) [7] with no great dissimilarities between the brain hemispheres. Although our unsupervised algorithm can obtain numerical results for other cases, the results may not be interpretable in the same way. In future, detection of these situations may lead to intelligent analysis of unusual feature or abnormalities.

For example, heads such as the one shown in Figure 10 are physiologically asymmetric to a large degree. Notice that the cosine harmonics have captured the principal symmetric shape features such as the broad frontal area, the low lateral convexity, and the roundness in the posterior region.

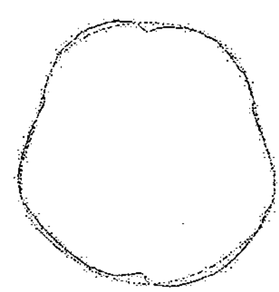

Figure 10: *Symmetry Description of an Asymmetric Shape* The head is noticeably asymmetric about its axis of least asymmetry (dark points). The cosine five-harmonic approximation (light points) captures only broad features, as intended.

The quantification of shape is simplified if the shape boundaries of a person's hemispheres have equal perimeter and radial occupancy. Figure 11 illustrates a situation where neither of these is true. Currently, the interpretation of our current algorithms in this situation is undefined.

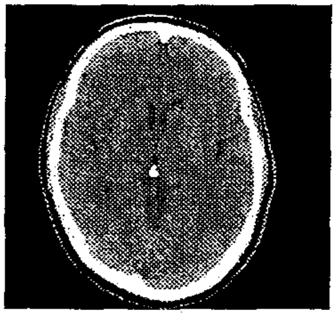

Figure 11: *Uncertain Interpretation* The patient's nose points to the top of the image in this orientation. Notice the relative positions of the hemispheres and structures such as the interhemispheric (central) fissure and frontal horns of the lateral ventricles.

7 Classification of Shape

We can classify shapes using harmonic coefficients, curvature [3], asymmetry, and error between the complete and low-frequency harmonic content.

The harmonic coefficients were found to be statistically Gaussian and, as predicted by Christopher (1974) [8], independent. As such, no correlation or 'clustering' was seen. However, superposition of harmonics leads to various typical shapes, shown in Figure 12. In general, the second harmonic is significant in heads that are much longer than they are wide. The third harmonic is significant in heads that have a broad posterior combined with a narrower anterior. The fourth and fifth harmonics capture convexity at the front and both sides.

It was found that degrees of asymmetry above 2.3 corresponded to patients with focal bone abnormalities, including foreign objects. It was also found to be indicative of mis-selected images (the bi-parietal slices were selected automatically by an unsupervised algorithm). Asymmetries above 1.0 corresponded with large visible imbalances (including differences in length) between the hemispheres. Asymmetries between 0 and 1.0 corresponded with typical shapes. The majority of cases fell into this latter category. No shape boundaries were found to have zero asymmetry. The mean was 0.54 and standard deviation was 0.5 for 528 cases.

It was found that the shape boundaries could be represented to within 3% by the use of only five cosine harmonics. Thus, each shape boundary can be quantified to this accuracy with only six parameters: the harmonics plus a size factor. By adding more harmonics, the shape boundaries can be quantified more accurately with little increase in the number of parameters. However, it was found that relating the magnitudes of the low-frequency harmonic coefficients alone did not enable automated discrimination of shape boundary appearance. Some past research has suggested that symmetry-axis lateral sampling [9] or eigenshape approaches [10] could be of value.

It was found that the curvature extrema can describe shape boundaries according to increasing outward curvature ('cups') or decreasing curvature, as well as describing big and small end discs as in Blum (1973) [11]. By calculating a chain of curvature features [12], the human-perceived shape can be classified and compared between cases. Regions of boundary shape with high or low informational content [13] can be described in this way. For the cases examined, exactly four chain segments were present except in nine cases that had six, eight, or nine points. It appeared that these extra points represented areas of low curvature with some cosine-wave artefacts.

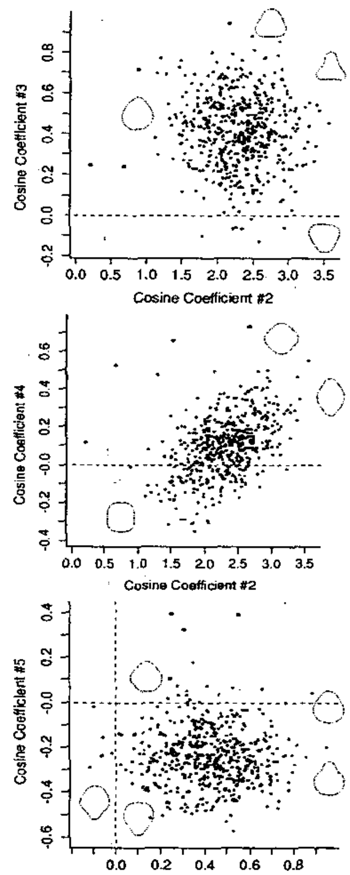

Figure 12: *Harmonic Planes* Pairs of harmonic coefficients are plotted in two dimensions. Hollow circles represent mis-acquired cross-sections. The dotted shapes show brain shape trends around the planes. There is no mistake in points lying on the unpopulated side of zero-point axes.

The position, magnitude, and relative ratios of shape boundary curvature were combined with harmonic coefficients to provide some tentative shape categories. Some non-medical shape boundary clusters were elucidated (see Table 1). It was found possible to retrieve similar-looking heads from a database using these criteria.

Description	Number of Cases Identified
Frontal: broad	180
Lateral Anterior: low convexity	258
Lateral: excessive convexity	57
Occipital: broad	115

Table 1: *Non-medical Curvature Classification* Brain images were categorised according to harmonic coefficients in conjunction with the ratios and locations of their five-harmonic curvature extrema.

8 Conclusions

It is found possible to quantitatively measure and approximate a person's cross-sectional brain shape using Fourier descriptors. While these techniques might not directly lead to statistical clusters or shape, they are robust against noise and can be used to infer broad brain shape. Curvature analysis of the Fourier-approximated shapes does lead to numerical categorisation corresponding to shape perceptions.

This study appears to be the first of its kind using CT data taken from a large number of living patients. The algorithm described is written in Java, and is one of a suite of programs being used for data analysis of CT brain scans.

9 Acknowledgements

This work was funded by the WA State Government Centres of Excellence Program—ARCME.

References

[1] A. Obenaus, C. J. Yong-Hing, K. A. Tong, and G. E. Sarty, "A reliable method for measurement and normalization of pediatric hippocampal volumes," *Pediatric Research*, vol. 50, no. 1, pp. 124–132, 2001.

[2] I. Emelyanova, K. Parker, L. Cala, R. Linggard, Y. Attikiouzel, K. Michalak, N. Hicks, P. Robbins, and F. Mastaglia, "Automatic Measurement of Brain Height from CT Scans," *WSEAS (The World Scientific and Engineering Academy and Society) Transactions on Circuits*, vol. 1, no. 1, pp. 165–168, 2002.

[3] W.-Y. Ma and B. S. Manjunath, "Netra: A toolbox for navigating large image databases," *Multimedia Systems*, vol. 7, no. 3, pp. 184–198, 1999.

[4] R. L. Anstey and D. Delmet, "Fourier analysis of zooecial shapes in fossil tubular bryozoans," *Geological Society of America Bulletin*, vol. 84, no. 5, pp. 1753–1764, 1973.

[5] Y. Rui, A. She, and T. Huang, "Modified fourier descriptors for shape representation – a practical approach," in *First International Workshop on Image Databases and Multi Media Search*, 1996.

[6] R. Tello, "Fourier descriptors for computer graphics," *IEEE Transactions on Systems, Man, and Cybernetics*, vol. 25, pp. 861–865, May 1995.

[7] L. A. Cala, G. W. Thickbroom, J. L. Black, D. W. K. Collins, and F. L. Mastaglia, "Brain density and cerebro-spinal fluid space size: CT of normal volunteers," *American Journal of Neuroradiology*, vol. 2, pp. 41–47, Jan–Feb 1981.

[8] R. A. Christopher and J. A. Waters, "Fourier series as a quantitative descriptor," *Journal of Paleontology*, vol. 48, pp. 697–709, 1974.

[9] H. Blum and R. Nagel, "Shape description using weighted symmetric axis features," *Pattern Recognition*, vol. 10, no. 3, pp. 167–180, 1978.

[10] N. McLeod, "Eigenshape analysis," *Paleobiology*, vol. 25, pp. 107–138, 1999.

[11] H. Blum, "Biological shape and visual science (part I)," *Journal of Theoretical Biology*, vol. 38, pp. 205–287, 1973.

[12] F. Leymarie and M. D. Levine, "Curvature morphology," Tech. Rep. TR-CIM-88-26, Centre for Intelligent Machines, McGill University, 1988.

[13] M. Leyton, "Symmetry-curvature duality," *Computer Vision Graphics and Image Processing*, vol. 38, pp. 327–341, 1987.